

Action Selection Learning for Multi-label Multi-view Action Recognition

Trung Thanh Nguyen
nguyent@cs.is.i.nagoya-u.ac.jp
Nagoya University, Nagoya, Japan
RIKEN, Kyoto, Japan

Takahiro Komamizu
taka-coma@acm.org
Nagoya University, Nagoya, Japan

Yasutomo Kawanishi
yasutomo.kawanishi@riken.jp
RIKEN, Kyoto, Japan
Nagoya University, Nagoya, Japan

Ichiro Ide
ide@i.nagoya-u.ac.jp
Nagoya University, Nagoya, Japan

Abstract

Multi-label multi-view action recognition aims to recognize multiple concurrent or sequential actions from untrimmed videos captured by multiple cameras. Existing work has focused on multi-view action recognition in a narrow area with strong labels available, where the onset and offset of each action are labeled at the frame-level. This study focuses on real-world scenarios where cameras are distributed to capture a wide-range area with only weak labels available at the video-level. We propose the method named **MultiASL (Multi-view Action Selection Learning)**, which leverages action selection learning to enhance view fusion by selecting the most useful information from different viewpoints. The proposed method includes a Multi-view Spatial-Temporal Transformer video encoder to extract spatial and temporal features from multi-viewpoint videos. Action Selection Learning is employed at the frame-level, using pseudo ground-truth obtained from weak labels at the video-level, to identify the most relevant frames for action recognition. Experiments in a real-world office environment using the MM-Office dataset demonstrate the superior performance of the proposed method compared to existing methods.

CCS Concepts

• **Computing methodologies** → **Computer vision tasks; Activity recognition and understanding.**

Keywords

Action Selection Learning, Event Detection, Multi-label, Multi-view Action Recognition.

ACM Reference Format:

Trung Thanh Nguyen, Yasutomo Kawanishi, Takahiro Komamizu, and Ichiro Ide. 2024. Action Selection Learning for Multi-label Multi-view Action Recognition. In *Proceedings of ACM Multimedia Asia (MMAAsia)*. ACM, New York, NY, USA, 7 pages. <https://doi.org/XXXXXXX.XXXXXXX>

Permission to make digital or hard copies of all or part of this work for personal or classroom use is granted without fee provided that copies are not made or distributed for profit or commercial advantage and that copies bear this notice and the full citation on the first page. Copyrights for components of this work owned by others than the author(s) must be honored. Abstracting with credit is permitted. To copy otherwise, or republish, to post on servers or to redistribute to lists, requires prior specific permission and/or a fee. Request permissions from permissions@acm.org.
MMAAsia, December 03–06, 2024, Auckland, New Zealand

© 2024 Copyright held by the owner/author(s). Publication rights licensed to ACM.
ACM ISBN 978-1-4503-XXXX-X/18/06
<https://doi.org/XXXXXXX.XXXXXXX>

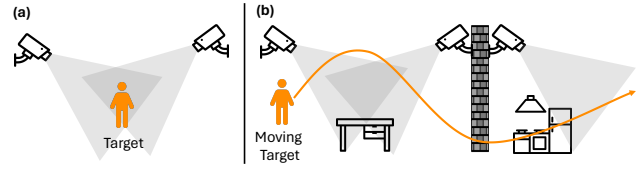


Figure 1: Configuration of multi-view settings. (a) Multiple cameras arranged to surround a target in a narrow area. (b) Multiple distributed cameras covering a wide-range area.

1 Introduction

Action recognition is an active research area in computer vision, garnering significant interest due to its wide range of applications, including surveillance [15], robotics [37], and video content analysis [25]. With the rapid advancements in multi-camera systems [24], there is an increasing need to capture and analyze actions from multiple viewpoints to obtain a comprehensive understanding.

Conventional single-view action recognition methods [12, 19, 34] are inherently limited by the perspective from which the action is observed, often resulting in incomplete understanding and potential misclassification of actions. In contrast, multi-view action recognition approaches integrate information from different viewpoints, providing a more holistic understanding of actions through complementary information. However, as shown in Figure 1a, current research [3, 29, 38, 41] primarily focuses on multi-camera setups surrounding a target in a narrow area. This setup is constrained for real-world scenarios where a target can move across a wide-range area. Figure 1b illustrates cameras distributed to capture a wide-range area. The success of multi-view action recognition lies in the effective joint representation of complementary information from different viewpoints. The challenge in a wide-range area is fusing information from various cameras, especially when some cameras may capture irrelevant information if the target is outside their view.

Typically, deep learning models for action recognition achieve the best results with strong labels, where the onset and offset of each action are annotated at the frame-level. However, such detailed annotation is costly for multiple cameras, and in many cases, only weak labels in the form of multi-label tags at the video-level are available [43, 44]. While some research [35, 50] has explored multi-label multi-view action recognition, they have primarily focused on multi-view setups in narrow areas, and the challenges of using

weak labels still need to be adequately addressed. Unlike previous works, this study addresses the challenges of action recognition in wide-range areas by focusing on multi-view fusion and multi-label recognition based on weak labels. We propose the MultiASL method, which employs action selection learning for multi-view action recognition to identify the most relevant actions using only video-level labels. This study makes the following contributions:

- We propose the Multi-view Spatial-Temporal Transformer video encoder to extract spatial and temporal features from videos, combined with Action Selection Learning (ASL) to identify useful frames for integrating information from multiple views using only video-level labels.
- We explore various multi-view fusion strategies (e.g., max pooling, mean pooling, sum, and concatenation) to determine the most effective fusion method. The findings show that max pooling consistently yields the best results.
- Experiments on real-world office environments using the MM-Office dataset [44] demonstrate the superior performance of the proposed MultiASL method compared to existing methods.

2 Related Work

Action Recognition. Advancements in action recognition have leveraged various deep learning techniques to improve the accuracy and robustness of identifying human actions in videos. Compared to image classification [10], action recognition depends on spatiotemporal features extracted from consecutive frames. Early attempts at video understanding used a combination of 2D Convolutional Neural Network (CNN) [16, 31, 39] or 3D CNN [1, 6, 42] to capture spatial and temporal information. Recently, with the success of Transformers [36] leading to the development of Vision Transformers (ViT) [8], researchers have proposed Transformer-based and ViT-based models for action recognition [2, 4, 7, 14] that effectively capture long-range spatiotemporal relationships, surpassing their convolutional counterparts.

Multi-view Action Recognition. The development of datasets with multi-view and multiple modalities (i.e., RGB, depth, and skeleton) [20, 30] has enabled recent progress in multi-view action recognition. Most research based on Skeleton methods [32, 33, 47] has received significant attention due to the availability of accurate 3D skeleton ground-truth. However, estimating an accurate 3D skeleton from videos without access to depth information is challenging. Besides that, to avoid dependence on the skeleton modality, some studies focus on RGB-based multi-view methods, proposing supervised contrastive learning [29] or an unsupervised representation learning framework [38] to learn a feature embedding robust to changes in viewpoint. However, current works typically utilize multiple views in a narrow area.

Multi-label Action Recognition. Recent research involves recognizing multiple actions performed simultaneously or sequentially in videos [27, 45]. Most studies focus on single-action recognition, employing a sigmoid activation function for the output to provide multi-label predictions [11, 48]. Other works introduce an actor-agnostic approach with a multi-modal query network to enhance multi-label action recognition [23]. Semi-supervised learning methods address class imbalance in multi-label classification [46], while

weakly-supervised learning aids in recognizing multiple actions with weak labels [40]. These advancements emphasize the importance of robust methods for handling multiple concurrent actions in diverse video datasets.

Multi-label Multi-view Action Recognition. While existing work has significantly contributed to multi-label and multi-view learning, the challenge of using weak labels has yet to be adequately addressed in [35, 50]. In these cases, videos have only video-level annotations without frame-level annotations. Moreover, in the context of distributed cameras covering a wide-range area, irrelevant views can significantly impact recognition accuracy when fusing information from multiple views. To address this challenge, we propose action selection learning at the frame-level using only video-level label for multi-view action recognition to reduce irrelevant information and enhance accuracy.

3 Methodology

Figure 2 shows the two main components of the proposed MultiASL method, which is trained in an end-to-end setting: Video Encoder (Figure 2a) and ASL (Figure 2b). The model processes a set of videos $\mathcal{V} = \{V_1, V_2, \dots, V_N\}$ from N views, represented as $V_i \in \mathbb{R}^{T \times D \times H \times W}$, where T is the number of frames, D is the number of channels, and H and W are the height and width, respectively. The Video Encoder extracts spatial and temporal features to predict actions at the video-level, while ASL uses the frame-level spatial and temporal features to select actions based on video-level labels. This approach addresses the challenge of irrelevant frames in multi-view feature fusion, outputting multi-label action predictions $A \in \{0, 1\}^C$, where C is the number of action classes.

3.1 Video Encoder

Figure 2a shows an overview of the Video Encoder used to extract spatial and temporal features from videos taken from N views. In the encoder, the Shared Spatial Encoder aims to extract detailed spatial features from each frame of the videos, capturing important visual information. This is followed by the Shared Temporal Transformer Encoder, which captures temporal dependencies to understand the sequence and progression of actions over time. Finally, the aggregated features from multiple views are used for video-level action prediction. Additionally, the frame-level spatial and temporal features are used for ASL.

3.1.1 Shared Spatial Encoder. Each video V_i from the i -th view ($i \in \{1, 2, \dots, N\}$) is processed by a spatial feature extractor, such as a Convolutional Neural Network (e.g., ResNet [13]) or Vision Transformer (ViT) [8]. This extractor processes each of the T frames of each video, capturing spatial features from each frame. The output of the spatial feature extractor for each view i is a set of spatial features, denoted as $F_i^{\text{Spatial}} \in \mathbb{R}^{T \times D_{\text{Spatial}}}$, where D_{Spatial} is the dimensionality of the extracted features.

3.1.2 Shared Temporal Transformer Encoder. The spatial features $F_i^{\text{Spatial}} \in \mathbb{R}^{T \times D_{\text{Spatial}}}$ for each view $i \in \{1, 2, \dots, N\}$ are then fed as input to a Temporal Transformer Encoder. This encoder is designed to capture temporal dependencies across the frames within each video, enabling the model to understand the sequence and progress of actions over time. The Temporal Transformer Encoder

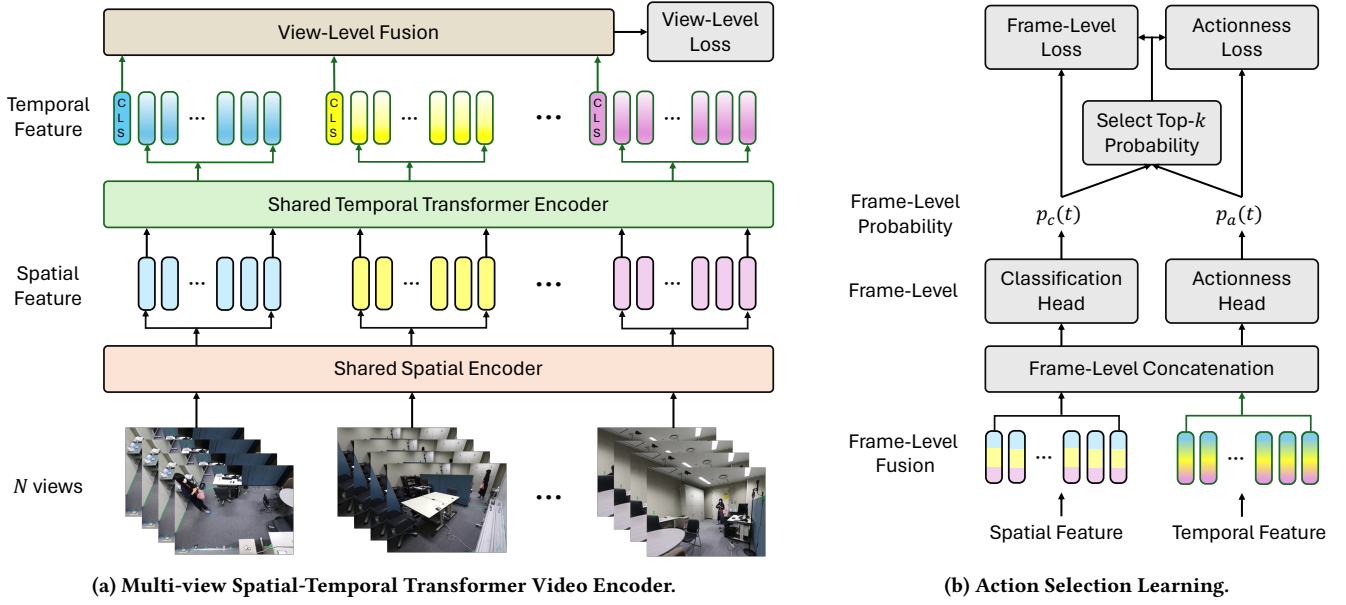


Figure 2: Overview of the proposed MultiASL model. The model takes videos from N different views as input and predicts multi-label actions. (a) Each video is processed by a Shared Spatial Encoder to extract spatial features, which are then fed into a Shared Temporal Transformer Encoder to capture temporal dependencies and generate temporal features. Finally, view-level features are aggregated for action recognition. (b) Frame-level spatial and temporal features are fused to select actions based on video-level labels.

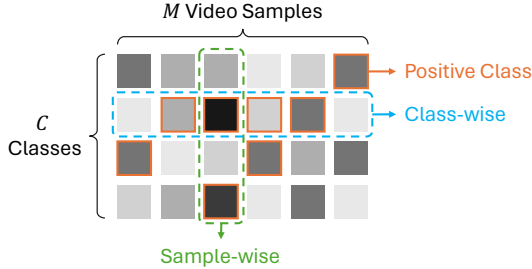


Figure 3: Logit matrix X for M video samples and C classes for Two-way multi-label loss [18].

leverages self-attention mechanisms [36] to weigh the importance of each frame relative to the others, effectively summarizing the temporal dynamics. The output of this process is a set of temporal features for each view, denoted as $F_i^{\text{Temporal}} \in \mathbb{R}^{T \times D_{\text{Temporal}}}$, where D_{Temporal} represents the dimensionality of these temporal features. Additionally, a classification token (CLS) is used within the transformer architecture to aggregate the information from all frames. The CLS token $F_i^{\text{CLS}} \in \mathbb{R}^{D_{\text{Temporal}}}$ is extracted at the output and is used to represent the entire video for video-level classification.

3.1.3 View-Level Classifier. We aggregate the video feature representations $F_i^{\text{CLS}} \in \mathbb{R}^{D_{\text{Temporal}}}$ from each view $i \in \{1, 2, \dots, N\}$ using fusion operation (e.g., max pooling, mean pooling, and sum). The view-level fused feature $F_{\text{View-fused}}$ is then passed through a linear layer for view-level classification. Typically, Binary Cross Entropy

(BCE) loss is commonly used in multi-label classification and discriminates samples for each class using a sigmoid function, which can be regarded as *class-wise* classification. However, BCE loss faces issues due to class imbalance, leading to suboptimal performance. Inspired by [18], we employ Two-way multi-label loss, which effectively exploits the discriminative characteristics through relative comparisons among classes and video samples. Figure 3 visualizes the logit matrix X for M video samples and C classes. The two-way loss for multi-label classification incorporates both the *sample-wise* and *class-wise* losses to enhance discrimination in both dimensions. The overall View-level loss is defined as:

$$\mathcal{L}_{\text{View-level}} = \mathcal{L}_{\text{Sample-wise}} + \alpha \mathcal{L}_{\text{Class-wise}}, \quad (1)$$

where α is a balancing parameter.

Sample-wise loss focuses on discriminating the positive and negative classes for each video sample as:

$$\mathcal{L}_{\text{Sample-wise}} = \frac{1}{M} \sum_{m=1}^M \text{softplus} \left(\log \sum_{n \in \mathcal{N}_m} e^{x_{S_n}} + \gamma \log \sum_{p \in \mathcal{P}_m} e^{-\frac{x_{S_p}}{\gamma}} \right),$$

where \mathcal{P}_m and \mathcal{N}_m denote the sets of positive and negative labels for the m -th video sample, respectively. Here, x_{S_n} and x_{S_p} represent the logits for the positive and negative classes, respectively. γ is a temperature parameter.

Class-wise loss focuses on discriminating the samples within each class as:

$$\mathcal{L}_{\text{Class-wise}} = \frac{1}{C} \sum_{c=1}^C \text{softplus} \left(\log \sum_{n \in \mathcal{N}_c} e^{x_{C_n}} + \gamma \log \sum_{p \in \mathcal{P}_c} e^{-\frac{x_{C_p}}{\gamma}} \right),$$

where \mathcal{P}_c and \mathcal{N}_c denote the sets of samples with positive and negative labels for the c -th class, respectively. Here, x_{C_n} and x_{C_p}

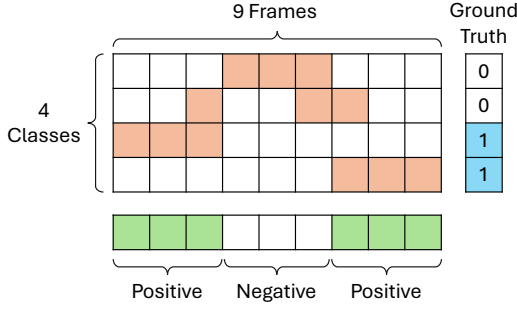


Figure 4: Example of generating pseudo ground-truth for actionness loss. The video consists of 9 frames and 4 video-level classes, with the ground-truth classes being 3 and 4. We select the top-3 predictions for each class (in orange). The positive class for frame-level is selected by taking the logical sum of the selected frames across the ground-truth video-level classes (in green).

represent the logits for the positive and negative samples within the class c , respectively. γ is a temperature parameter.

3.2 Action Selection Learning

Figure 2b shows an overview of ASL. The input for ASL consists of the spatial feature $F_i^{\text{Spatial}} \in \mathbb{R}^{T \times D_{\text{Spatial}}}$ and the temporal feature $F_i^{\text{Temporal}} \in \mathbb{R}^{T \times D_{\text{Temporal}}}$ from each view $i \in \{1, 2, \dots, N\}$. Each frame in the spatial and temporal feature is aggregated at the frame level using fusion operation (e.g., max pooling, mean pooling, and sum). The resulting frame-level fused features are $F_{\text{Frame-fused}}^{\text{Spatial}} \in \mathbb{R}^{D_{\text{Spatial}}}$ and $F_{\text{Frame-fused}}^{\text{Temporal}} \in \mathbb{R}^{D_{\text{Temporal}}}$. These fused spatial and temporal features are then concatenated to obtain the combined feature $F_{\text{Frame-fused}}^{\text{S-T}} \in \mathbb{R}^{D_{\text{S-T}}}$, where $D_{\text{S-T}} = D_{\text{Spatial}} + D_{\text{Temporal}}$.

ASL aims to learn to select actions at the frame-level, for which we design two classifiers: Frame-level classifier and Actionness classifier. The features $F_{\text{Frame-fused}}^{\text{S-T}}$ are fed into the classification head and actionness head to obtain the frame-level probability of class $p_c(t)$ and actionness $p_a(t)$ for $t \in \{1, \dots, T\}$. The Frame-level classifier aims to predict the video class based on an aggregate of top- k frame probabilities using the Multiple Instance Learning (MIL) [5] approach, with the top- k probability being the sum of $p_c(t)$ and $p_a(t)$. On the other hand, the Actionness classifier aims to predict a binary logit for each frame, indicating whether it is an action or non-action based on the video-level class. Since we only have video-level labels, we select the top- k probabilities of $p_c(t)$ and $p_a(t)$ to serve as the ground-truth for actionness loss.

3.2.1 Frame-Level Classifier. For class probability $p_c(t)$ over $t = \{1, \dots, T\}$ frames, the MIL approach is commonly employed to train the classifier when only video-level labels are available. This approach selects the top- k probabilities for each class to aggregate the highest frame-level probabilities and make video-level predictions. We denote the set of top- k probabilities for each class as:

$$\mathcal{T}^c = \underset{\substack{\mathcal{T} \subseteq \{1, \dots, T\} \\ \text{s.t. } |\mathcal{T}|=k}}{\operatorname{argmax}} \sum_{t \in \mathcal{T}} (p_c(t) + p_a(t)), \quad (2)$$

where $\mathcal{T} \subseteq \{1, \dots, T\}$ represents a subset of frames from the total T frames, $|\mathcal{T}| = k$ means that the subset \mathcal{T} contains k frames, $p_c(t)$ is the class probability, and $p_a(t)$ is the actionness probability. Then the video-level class probability can be selected by aggregation (e.g., mean pooling) using \mathcal{T}^c as:

$$p_c = \text{AGGREGATION} \left(\frac{1}{k} \sum_{t \in \mathcal{T}^c} p_c(t) \right). \quad (3)$$

Finally, similar to the View-level loss in Eq. 1, we employ the Two-way multi-label loss to obtain the Frame-level loss $\mathcal{L}_{\text{Frame-level}}$.

3.2.2 Actionness Classifier. To reduce the impact of irrelevant frames in a video, we propose the actionness classifier to identify which frames contain actions and which do not, denoted by $p_a(t)$ for $t \in \{1, \dots, T\}$. However, since only video-level labels are available, it is challenging to learn this through strong label supervised learning. To address this issue, we select positive and negative frames based on the top- k predictions. As shown in Eq. 2, we obtain the set of top- k predictions \mathcal{T}^c . We use the video-level ground-truth classes to select positive frame \mathcal{T}_{Pos} and negative frame \mathcal{T}_{Neg} by taking the logical sum of the top- k predictions \mathcal{T}^c for the positive class across the ground-truth classes. An example of the frame selection strategy is visualized in Figure 4.

Since the Actionness classifier is trained based on pseudo ground-truth derived from prediction probabilities, this leads to challenges during early training when action classification accuracy is poor and the top- k selections are not accurate. Consequently, the pseudo ground-truth can be very noisy, making it difficult for the model to converge. To address this problem, following [22] and [49], we employ the Generalized Cross Entropy Loss as:

$$\mathcal{L}_{\text{Actionness}} = \frac{1}{|\mathcal{T}_{\text{Pos}}|} \sum_{t \in \mathcal{T}_{\text{Pos}}} \frac{1 - (p_a(t))^q}{q} + \frac{1}{|\mathcal{T}_{\text{Neg}}|} \sum_{t \in \mathcal{T}_{\text{Neg}}} \frac{1 - (1 - p_a(t))^q}{q}, \quad (4)$$

where \mathcal{T}_{Pos} and \mathcal{T}_{Neg} denote the sets of positive and negative frames, respectively, and $0 < q \leq 1$ determines the noise tolerance.

3.3 Learning Objectives

The learning objectives of the proposed MultiASL model encompass three main components: View-level loss, Frame-level loss, and Actionness loss. The overall loss function is defined as:

$$\mathcal{L}_{\text{Overall}} = \mathcal{L}_{\text{View-level}} + \beta_1 \mathcal{L}_{\text{Frame-level}} + \beta_2 \mathcal{L}_{\text{Actionness}}, \quad (5)$$

where β_1 and β_2 are weighting factors. While the View-level loss facilitates multi-class prediction by aggregating all features within the multi-view videos, the fused features often contain irrelevant frames, which can hinder the learning process. The ASL aims to remove these irrelevant frames by training the Actionness classifier based on pseudo ground-truth obtained from frame-level predictions. This approach ensures that the model focuses on the most informative frames, thereby enhancing the robustness of the proposed method.

Table 1: Comparison of the proposed MultiASL and other methods. The best and second-best results are highlighted in bold and underlined text, respectively.

Method	Backbone	View-level Fusion Strategy							
		Max		Mean		Sum		Concat	
		mAP _C	mAP _S	mAP _C	mAP _S	mAP _C	mAP _S	mAP _C	mAP _S
MultiTrans [44]	Resnet18	82.10	89.15	82.70	90.09	82.28	89.57	81.04	89.27
MultiTrans [44]	Resnet34	82.93	89.47	83.57	90.88	83.03	90.74	81.41	89.44
MultiTrans [44]	ViT	84.47	90.64	84.73	91.08	82.56	86.66	80.40	87.71
Query2Label [21]	CLIP	22.93	51.14	20.45	50.42	26.45	50.79	22.88	50.99
Query2Label [21]	ViT	35.62	51.19	35.74	51.19	37.38	51.00	24.05	50.36
ConViT [9]	ViT	81.92	89.20	80.27	87.54	81.96	88.93	80.09	88.52
TimeSformer [4]	ViT	79.28	86.92	70.76	82.31	79.33	87.66	68.61	82.63
ViViT [2]	ViT	75.95	87.25	71.18	80.97	70.46	81.93	70.11	79.97
MultiASL (Proposed)	Resnet18	86.12	90.61	<u>86.71</u>	<u>91.81</u>	<u>86.22</u>	92.38	<u>84.83</u>	<u>90.11</u>
	Resnet34	<u>86.55</u>	93.06	83.34	90.29	86.06	93.32	82.19	88.99
	ViT	88.05	<u>91.91</u>	87.01	92.20	87.36	<u>92.95</u>	86.33	90.16

4 Experiments

4.1 Experimental Conditions

4.1.1 Dataset. We utilize the MM-Office dataset [44], which comprises recordings from multiple cameras positioned at the four corners of an office room. Within this setting, 1 to 3 people engage in various daily work activities, classified into 12 distinct classes. We use 2,816 videos captured from four distributed cameras. Each video is annotated with multi-label tags, and the average length of the dataset is 43.25 seconds. The dataset contains 1,392 events and has an unbalanced number of events across classes. To create the training and test sets, we use the Iterative Stratification strategy [28] for multi-label data with a 70:30 ratio, ensuring that all action classes are adequately represented in both subsets.

For the experiments, we extract a fixed number of T frames at a sampling rate of 2.5 FPS. During the training phase, from the total frames of the original video, we generate a perturbed sequence of frame indices for a given length T . This sequence is based on uniform sampling, with random adjustments to ensure that the index covers the entire length, serving as a data augmentation method for robust training. During testing, we use uniform sampling to ensure that the index remains consistent across every test.

4.1.2 Evaluation Metrics. Following Kobayashi et al. [18], we evaluate performance using the two metrics below:

- **mAP_C** (macro-averaged metric): Mean average precision is computed for each class and then aggregated across *classes*. This is a primary metric in multi-label classification.
- **mAP_S** (micro-averaged metric): Mean average precision is measured over *samples*. This is a standard metric for single-label classification.

4.1.3 Comparison Methods. To evaluate the effectiveness of the proposed method, we compare it with the following methods:

- **MultiTrans [44]:** Multi-view and multi-modal event detection by utilizing Transformer-based multi-sensor fusion. It integrates data from distributed sensors through stacked

Transformer blocks, effectively combining features from different viewpoints and modalities.

- **Query2Label [21]:** Leverages Transformer decoders to query class labels for multi-label classification, utilizing CLIP [26] features for vision and language queries.
- **ConViT [9]:** Improving ViT with soft convolutional inductive biases. We modified ConViT with a Temporal Transformer Encoder to learn the temporal relationships in videos.
- **TimeSformer [4] and ViViT [2]:** Transformer-based architectures for video classification, applying self-attention mechanisms across spatial and temporal dimensions to capture complex video dynamics.

4.1.4 Models & Hyperparameters. We implement the proposal MultiASL method as detailed in Section 3¹. The input to the model consists of 4 views captured from cameras with a fixed frame of $T = 50$ and a resolution of $3 \times 224 \times 224$. For the Spatial Encoder, we employ different backbones including ResNet18 [13], ResNet34 [13], and ViT [8]. For the Temporal Transformer Encoder, we use one Transformer Encoder [36] layer with four heads, each having a dimension of 128. The balancing parameter α and temperature parameter γ in Eq. 1 are set to 1 and 4, respectively. The noise tolerance q in Eq. 4 is set to 0.7, where q being close to 1 makes the model more tolerant to deviations from the ground-truth. The parameters β_1 and β_2 in Eq. 5 are both set to 1 for simplicity. The parameter k for selecting the top- k probabilities is set to $k = T/8$. We employ multiple methods for View-level fusion, including max pooling, mean pooling, sum, and concatenation, while for Frame-level fusion, we use max pooling. For optimization, we use the Adam optimizer [17] with an initial learning rate set at 10^{-4} and a weight decay of 5.0×10^{-4} until convergence. The maximum number of epochs is fixed at 50 with a batch size of 8. All experiments are performed on a machine equipped with an AMD EPYC 7402P 24-core processor and an NVIDIA A6000 GPU.

¹The source code is available at <https://github.com/thanhff/MultiASL/>.

Table 2: Multi-label single-view action recognition. The average precision of each class is reported, with the best results are highlighted in bold.

Setting	Eat	Tele	Chat	Meeting	Takeout	Prepare	Handout	Enter	Exit	Stand up	Sit down	Phone	Average
All view	90.67	98.22	96.62	97.84	98.27	98.47	56.66	98.80	95.37	72.52	77.66	75.53	88.05
View 1	79.77	98.96	96.06	97.08	97.54	98.02	45.34	99.17	93.95	52.21	73.13	65.60	83.07
View 2	83.96	98.07	93.98	92.25	98.09	96.27	46.21	98.53	87.26	58.26	71.62	79.21	83.64
View 3	71.90	93.12	82.68	54.63	99.25	86.71	39.22	95.32	85.58	49.07	62.12	70.21	74.15
View 4	47.06	85.23	68.81	94.65	53.48	79.93	25.28	34.42	29.89	55.55	56.68	73.90	58.74

Table 3: Impact of different loss components. The best results are highlighted in bold.

View-level loss	Frame-level loss	Actionness loss	mAP _C	mAP _S
✓	✓	✓	88.05	91.91
✓	✓		85.90	90.99
✓			84.04	89.90
	✓	✓	84.30	89.12
	✓		81.65	87.82

4.2 Results

Table 1 shows the results of the proposed MultiASL compared to other methods. MultiASL demonstrates superior performance across various backbone architectures (i.e., Resnet18, Resnet34, and ViT) and view-level fusion strategies (i.e., max pooling, mean pooling, sum, and concatenation) in terms of mAP_C and mAP_S. Notably, MultiASL with ResNet34 and ViT backbones consistently achieves the highest mAP. View-level fusion with max-pooling achieves the best results compared to other fusion strategies. With the ViT backbone, MultiASL achieves the best results with mAP_C of 88.05% and mAP_S of 91.91% using max pooling fusion, outperforming the MultiTrans, Query2Label, ConViT, TimeSformer, and ViViT models. These results demonstrate the robustness and effectiveness of MultiASL, with the ASL effectively selecting the action frames while reducing irrelevant information, thus enhancing accuracy.

4.3 Ablation Study

We conduct a series of excision experiments as part of an ablation study to evaluate the effectiveness of the MultiASL, using ViT as the spatial feature extractor and max-pooling for view-level fusion.

4.3.1 Multi-label Single-view Action Recognition. To demonstrate the effectiveness of the proposed multi-view fusion, we evaluated single-view input settings as shown in Table 2. The results indicate that single-view settings generally perform worse compared to multi-view fusion. Views 1 and 2 provide relatively higher accuracy due to their advantageous positioning and angles, capturing the most frequently occurring actions. Conversely, views 3 and 4 exhibit lower accuracy due to the distributed camera setup, where views overlap but do not focus around the target, causing some actions not visible from those views. The results also show that instantaneous actions such as “Stand up”, “Sit down”, and “Handout” are challenging to detect, suggesting these actions might occur in

brief moments easily missed by a single view. Moreover, view 2 shows superior results for the “Phone” action due to its proximity to the desk phone. On the other hand, view 4 performs worst in the “Enter” and “Exit” actions because the camera’s direction is not directly towards the door. These results demonstrate that integrating all views enhances accuracy by allowing information from different views to complement each other.

4.3.2 Impact of Different Loss Components. Table 3 shows the impact of different loss components on the performance of the proposed method. The full model achieves the highest performance. Removing the Actionness loss results in a slight performance drop, indicating its importance in improving prediction accuracy by identifying which frames contain actions. Further removing the Frame-level loss causes a greater drop in performance, demonstrating the critical role of ASL in overall accuracy. When only the Frame-level and Actionness losses are used, the model still performs well, but it is clear that the View-level loss is essential for achieving optimal performance. Lastly, the absence of both the View-level and Actionness losses results in the lowest performance, due to the difficulty in selecting top-*k* predictions to determine the video-level class.

5 Conclusion and Discussion

This study proposed the MultiASL method for enhancing multi-label multi-view action recognition using only video-level labels. By employing a Multi-view Spatial-Temporal Transformer video encoder and Action Selection Learning, the proposed approach effectively identifies and integrates relevant frames from multiple viewpoints. Various fusion strategies are explored to optimize the integration of information from different views. The experimental results on the real-world office environments offered by the MM-Office dataset demonstrate the robustness and accuracy of the MultiASL method, significantly outperforming existing methods.

Limitations and future work: In this study, we experimented with fixed hyper-parameters (i.e., top-*k* probabilities), leading to the need for future research to explore the impact of varying these hyper-parameters to optimize performance. Additionally, MultiASL relies solely on camera visual information, potentially missing contextual information from other modalities such as audio. Integrating multi-modal data could significantly enhance the robustness and accuracy of multi-label multi-view action recognition.

Acknowledgment

This work was partly supported by JSPS KAKENHI JP21H03519 and JP24H00733.

References

- [1] ALFAIFI, R., AND ARTOLI, A. M. Human action prediction with 3D-CNN. *SN Computer Science* 1, 5 (2020), 286.
- [2] ARNAB, A., DEGHANI, M., HEIGOLD, G., SUN, C., LUČIĆ, M., AND SCHMID, C. ViViT: A video vision transformer. In *Proceedings of the 18th IEEE/CVF International Conference on Computer Vision* (2021), pp. 6836–6846.
- [3] BAI, Y., TAO, Z., WANG, L., LI, S., YIN, Y., AND FU, Y. Collaborative attention mechanism for multi-view action recognition. *Computing Research Repository arXiv Preprints*, arXiv:2009.06599 (2020).
- [4] BERTASIO, G., WANG, H., AND TORRESANI, L. Is space-time attention all you need for video understanding? In *Proceedings of the 38th International Conference on Machine Learning* (2021), pp. 813–824.
- [5] CARBONNEAU, M.-A., CHEPLYGINA, V., GRANGER, E., AND GAGNON, G. Multiple instance learning: A survey of problem characteristics and applications. *Pattern Recognition* 77 (2018), 329–353.
- [6] CHEN, C.-F. R., PANDA, R., RAMAKRISHNAN, K., FERIS, R., COHN, J., OLIVA, A., AND FAN, Q. Deep analysis of CNN-based spatio-temporal representations for action recognition. In *Proceedings of the 2021 IEEE/CVF Conference on Computer Vision and Pattern Recognition* (2021), pp. 6165–6175.
- [7] DOSHI, K., AND YILMAZ, Y. Semantic video transformer for robust action recognition. In *Proceedings of the 2023 IEEE Conference on Dependable and Secure Computing* (2023), pp. 1–5.
- [8] DOSOVITSKIY, A., BEYER, L., KOLESNIKOV, A., WEISSENBORN, D., ZHAI, X., UNTERTHINER, T., DEGHANI, M., MINDERER, M., HEIGOLD, G., GELLY, S., USZKOREIT, J., AND HOULSBY, N. An image is worth 16x16 words: Transformers for image recognition at scale. *Computing Research Repository arXiv Preprints*, arXiv:2010.11929 (2020).
- [9] D’ASCOLI, S., TOUVRON, H., LEAVITT, M. L., MORCOS, A. S., BIROLI, G., AND SAGUN, L. ConViT: Improving vision transformers with soft convolutional inductive biases. In *Proceedings of the 38th International Conference on Machine Learning* (2021), pp. 2286–2296.
- [10] ELNGAR, A. A., ARAFA, M., FATHY, A., MOUSTAFA, B., MAHMOUD, O., SHABAN, M., AND FAWZY, N. Image classification based on CNN: A survey. *Journal of Cybersecurity and Information Management* 6, 1 (2021), 18–50.
- [11] FEICHTENHOFER, C., FAN, H., MALIK, J., AND HE, K. Slowfast networks for video recognition. In *Proceedings of the 17th IEEE/CVF International Conference on Computer Vision* (2019), pp. 6202–6211.
- [12] GUPTA, P., THATIPELLI, A., AGGARWAL, A., MAHESHWARI, S., TRIVEDI, N., DAS, S., AND SARVADEVBHATLA, R. K. Quo vadis, skeleton action recognition? *International Journal of Computer Vision* 129, 7 (2021), 2097–2112.
- [13] HE, K., ZHANG, X., REN, S., AND SUN, J. Deep residual learning for image recognition. In *Proceedings of the 2016 IEEE Conference on Computer Vision and Pattern Recognition* (2016), pp. 770–778.
- [14] HONG, Y., KIM, M. J., LEE, I., AND YOO, S. B. Fluxformer: Flow-guided duplex attention transformer via spatio-temporal clustering for action recognition. *IEEE Robotics and Automation Letters* 8, 10 (2023), 6411–6418.
- [15] KHAN, M. A., JAVED, K., KHAN, S. A., SABA, T., HABIB, U., KHAN, J. A., AND ABBASI, A. A. Human action recognition using fusion of multiview and deep features: an application to video surveillance. *Multimedia Tools and Applications* 83, 5 (2024), 14885–14911.
- [16] KIM, J.-H., AND WON, C. S. Action recognition in videos using pre-trained 2D convolutional neural networks. *IEEE Access* 8 (2020), 60179–60188.
- [17] KINGMA, D. P., AND BA, J. Adam: A method for stochastic optimization. *Computing Research Repository arXiv Preprints*, arXiv:1412.6980 (2014).
- [18] KOBAYASHI, T. Two-way multi-label loss. In *Proceedings of the 2023 IEEE/CVF Conference on Computer Vision and Pattern Recognition* (2023), pp. 7476–7485.
- [19] KONG, Y., AND FU, Y. Human action recognition and prediction: A survey. *International Journal of Computer Vision* 130, 5 (2022), 1366–1401.
- [20] LIU, J., SHAHROUDY, A., PEREZ, M., WANG, G., DUAN, L.-Y., AND KOT, A. C. NTU RGB+D 120: A large-scale benchmark for 3D human activity understanding. *IEEE Transactions on Pattern Analysis and Machine Intelligence* 42, 10 (2019), 2684–2701.
- [21] LIU, S., ZHANG, L., YANG, X., SU, H., AND ZHU, J. Query2Label: A simple transformer way to multi-label classification. *Computing Research Repository arXiv Preprints*, arXiv:2107.10834 (2021).
- [22] MA, J., GORTI, S. K., VOLKOV, M., AND YU, G. Weakly supervised action selection learning in video. In *Proceedings of the 2021 IEEE/CVF Conference on Computer Vision and Pattern Recognition* (2021), pp. 7587–7596.
- [23] MONDAL, A., NAG, S., PRADA, J. M., ZHU, X., AND DUTTA, A. Actor-agnostic multi-label action recognition with multi-modal query. In *Proceedings of the 2023 IEEE/CVF International Conference on Computer Vision* (2023), pp. 784–794.
- [24] OLAGOKE, A. S., IBRAHIM, H., AND TEOH, S. S. Literature survey on multi-camera system and its application. *IEEE Access* 8 (2020), 172892–172922.
- [25] PAREEK, P., AND THAKKAR, A. A survey on video-based human action recognition: recent updates, datasets, challenges, and applications. *Artificial Intelligence Review* 54, 3 (2021), 2259–2322.
- [26] RADFORD, A., KIM, J. W., HALLACY, C., RAMESH, A., GOH, G., AGARWAL, S., SASTRY, G., ASKELL, A., MISHKIN, P., CLARK, J., ET AL. Learning transferable visual models from natural language supervision. In *Proceedings of the 38th International Conference on Machine Learning* (2021), pp. 8748–8763.
- [27] RAY, J., WANG, H., TRAN, D., WANG, Y., FEISZLI, M., TORRESANI, L., AND PALURI, M. Scenes-objects-actions: A multi-task, multi-label video dataset. In *Proceedings of the 15th European Conference on Computer Vision* (2018), vol. 11218(14), pp. 660–676.
- [28] SECHIDIS, K., TSOUMAKAS, G., AND VLAHAVAS, I. On the stratification of multi-label data. In *Proceedings of the 2011 Machine Learning and Knowledge Discovery in Databases: European Conference* (2011), pp. 145–158.
- [29] SHAH, K., SHAH, A., LAU, C. P., DE MELO, C. M., AND CHELLAPPA, R. Multi-view action recognition using contrastive learning. In *Proceedings of the 2023 IEEE/CVF Winter Conference on Applications of Computer Vision* (2023), pp. 3381–3391.
- [30] SHAHROUDY, A., LIU, J., NG, T.-T., AND WANG, G. NTU RGB+D: A large scale dataset for 3D human activity analysis. In *Proceedings of the 2016 IEEE Conference on Computer Vision and Pattern Recognition* (2016), pp. 1010–1019.
- [31] SHEN, Z., WU, X.-J., AND KITTLER, J. 2D progressive fusion module for action recognition. *Image and Vision Computing* 109 (2021), 104122.
- [32] SHI, L., ZHANG, Y., CHENG, J., AND LU, H. Decoupled spatial-temporal attention network for skeleton-based action-gesture recognition. In *Proceedings of the 15th Asian Conference on Computer Vision* (2020), vol. 12626(5), pp. 38–53.
- [33] SHI, L., ZHANG, Y., CHENG, J., AND LU, H. Adasgn: Adapting joint number and model size for efficient skeleton-based action recognition. In *Proceedings of the 18th IEEE/CVF International Conference on Computer Vision* (2021), pp. 13413–13422.
- [34] SUN, Z., KE, Q., RAHMANI, H., BENNAMOUN, M., WANG, G., AND LIU, J. Human action recognition from various data modalities: A review. *IEEE Transactions on Pattern Analysis and Machine Intelligence* 45, 3 (2022), 3200–3225.
- [35] TAN, Q., YU, G., DOMENICONI, C., WANG, J., AND ZHANG, Z. Incomplete multi-view weak-label learning. In *Proceedings of the 27th International Joint Conference on Artificial Intelligence* (2018), pp. 2703–2709.
- [36] VASWANI, A., SHAZEER, N., PARMAR, N., USZKOREIT, J., JONES, L., GOMEZ, A. N., KAISER, L., AND POLOSUKHIN, I. Attention is all you need. *Advances in Neural Information Processing Systems* 30 (2017), 6000–6010.
- [37] VORONIN, V., ZHDANOVA, M., SEMENISHCHEV, E., ZELENISKII, A., CEN, Y., AND AGALAN, S. Action recognition for the robotics and manufacturing automation using 3-D binary micro-block difference. *The International Journal of Advanced Manufacturing Technology* 117 (2021), 2319–2330.
- [38] VYAS, S., RAWAT, Y. S., AND SHAH, M. Multi-view action recognition using cross-view video prediction. In *Proceedings of the 16th European Conference on Computer Vision* (2020), vol. 12372(27), pp. 427–444.
- [39] WANG, J., LU, H., ZHANG, Y., MA, F., AND HU, M. Temporal factorized bilinear modules with 2D CNN for action recognition in videos. In *Proceedings of the 7th International Conference on Computer and Communication Systems* (2022), pp. 261–266.
- [40] WANG, Q., AND CHEN, K. Multi-label zero-shot human action recognition via joint latent ranking embedding. *Neural Networks* 122 (2020), 1–23.
- [41] WANG, Q., SUN, G., DONG, J., WANG, Q., AND DING, Z. Continuous multi-view human action recognition. *IEEE Transactions on Circuits and Systems for Video Technology* 32, 6 (2021), 3603–3614.
- [42] WU, H., MA, X., AND LI, Y. Spatiotemporal multimodal learning with 3D CNNs for video action recognition. *IEEE Transactions on Circuits and Systems for Video Technology* 32, 3 (2021), 1250–1261.
- [43] YASUDA, M., HARADA, N., OHISHI, Y., SAITO, S., NAKAYAMA, A., AND ONO, N. Guided masked self-distillation modeling for distributed multimedia sensor event analysis. *Computing Research Repository arXiv Preprints*, arXiv:2404.08264 (2024).
- [44] YASUDA, M., OHISHI, Y., SAITO, S., AND HARADA, N. Multi-view and multi-modal event detection utilizing transformer-based multi-sensor fusion. In *Proceedings of the 47th IEEE International Conference on Acoustics, Speech and Signal Processing* (2022), pp. 4638–4642.
- [45] YEUNG, S., RUSSAKOVSKY, O., JIN, N., ANDRILUKA, M., MORI, G., AND FEI-FEI, L. Every moment counts: Dense detailed labeling of actions in complex videos. *International Journal of Computer Vision* 126 (2018), 375–389.
- [46] ZHANG, H., ZHAO, X., AND WANG, D. Semi-supervised learning for multi-label video action detection. In *Proceedings of the 30th ACM International Conference on Multimedia* (2022), pp. 2124–2134.
- [47] ZHANG, P., LAN, C., XING, J., ZENG, W., XUE, J., AND ZHENG, N. View adaptive neural networks for high performance skeleton-based human action recognition. *IEEE Transactions on Pattern Analysis and Machine Intelligence* 41, 8 (2019), 1963–1978.
- [48] ZHANG, Y., LI, X., AND MARSIC, I. Multi-label activity recognition using activity-specific features and activity correlations. In *Proceedings of the 2021 IEEE/CVF Conference on Computer Vision and Pattern Recognition* (2021), pp. 14625–14635.
- [49] ZHANG, Z., AND SABUNCU, M. Generalized cross entropy loss for training deep neural networks with noisy labels. *Advances in Neural Information Processing Systems* 31 (2018), 8792–8802.
- [50] ZHAO, D., GAO, Q., LU, Y., AND SUN, D. Non-aligned multi-view multi-label classification via learning view-specific labels. *IEEE Transactions on Multimedia* 25 (2023), 7235–7247.